

## DESIGN OF THE LABORATORY STAND FOR TESTING VEHICLE SUSPENSIONS

### SUMMARY

*This paper is devoted to the designing of the laboratory stand for testing car vehicle suspensions. Main parts of the laboratory setup are as follows: a frame construction with vehicle suspension elements, an electro-hydraulic shaker, a hydraulic power supply unit and a measurement and control system. This work provides preliminary analysis of the laboratory setup such as static analysis and dynamic simulations of the system. Results of the calculations were used in the designing process of the laboratory setup.*

**Keywords:** vehicle suspension, laboratory stand, quarter car

### PROJEKT STANOWISKA LABORATORYJNEGO DO TESTOWANIA ZAWIESZEŃ SAMOCHODOWYCH

*Niniejsza praca jest poświęcona projektowi stanowiska laboratoryjnego do testowania zawiesznień samochodowych. Główne elementy stanowiska to: konstrukcja ramowa wraz z elementami badanego zawieszenia, elektro-hydrauliczny wzbudnik drgań, stacja zasilania hydraulicznego oraz jednostka pomiarowo-sterująca. W ramach obliczeń wykonano analizę statyczną oraz przeprowadzono symulacje dynamiki projektowanego układu. Otrzymane wyniki zostaną wykorzystane w kolejnych pracach projektowych.*

**Słowa kluczowe:** zawieszenie samochodowe, stanowisko laboratoryjne, ćwiartka samochodu

### 1. INTRODUCTION

The design of vehicle suspensions is a compromise between driving safety and driving comfort (Reimpel 2000). Fast evolution of vehicle suspension systems makes possible to decrease the vibration transmission from the wheel to the body and provides better ride quality, handling and road holding. The development of vehicles requires designing the advanced laboratory stands for testing various kinematic structures of vehicle suspensions and various control algorithms. An example laboratory setup was introduced in (Langdon 2007) where authors considered a quarter car test rig. The new laboratory stand was built and investigated. Some control algorithms were applied to this new setup to carry out preliminary experiments and evaluation. A new quarter car test rig was also presented in (Mohd 2008). This work includes simulations as well as experimental studies of the laboratory stand. Another applications of the laboratory stands were introduced in (Yoshimura 2001) and (Teramura 2005). Laboratory setups considered in these works comprise sprung and unsprung masses connected with suspension elements. The sprung mass represents quarter car body and the unsprung mass represents a car wheel. Authors considered some active control algorithms and compared simulation and experimental results.

This paper contains some technical assumptions and preliminary analysis which were done as a part of the project of the laboratory stand for testing vehicle suspensions. Parameters of the vehicle suspension were determined. Mathema-

tical model of the suspension system was prepared and used for simulations. Results of calculations and simulations will be used in the next stages of the project.

### 2. DESCRIPTION OF THE LABORATORY STAND

At the beginning of the design process some assumptions were done. The laboratory setup (Fig. 1) will consist of: a frame construction 1, a moveable frame 2, a vehicle suspension system 3, an electrohydraulic shaker 4, a hydraulic power supply unit 5, a measurement and control system 6. In accordance with the assumptions (Fig. 1) the moveable frame 2 is connected with the steel construction 1 by linear bearings in a way to make possible its longitudinal move along the steel construction 1. The elements of vehicle suspension system 3 are fixed to the moveable frame 2 and connected with the car wheel. The car wheel is placed on the top of the electrohydraulic shaker 4. The hydraulic power supply is intended to deliver hydraulic fluid to the shaker system. Measurement and control device 6 will consist of all necessary electric and electronic equipment to steering the system and gathering data.

The laboratory stand is intended to test single independent car suspensions. For further calculations and simulations the elements of a front MacPherson strut of Ford Focus were investigated.

A simplified model of the vehicle suspension with the car wheel and the moveable frame 2 is shown in Figure 2.

\* AGH University of Science and Technology, Faculty of Mechanical Engineering and Robotics, Department of Process Control, al. A. Mickiewicza 30, 30-059 Krakow; jkowal@agh.edu.pl

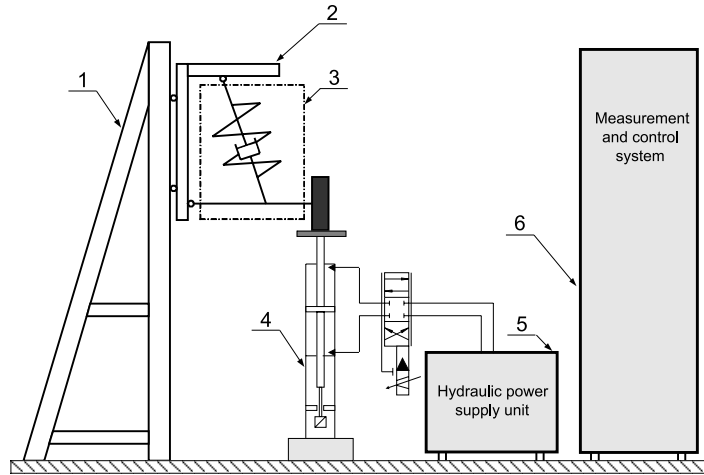


Fig. 1. Scheme of the laboratory stand for testing vehicle suspensions

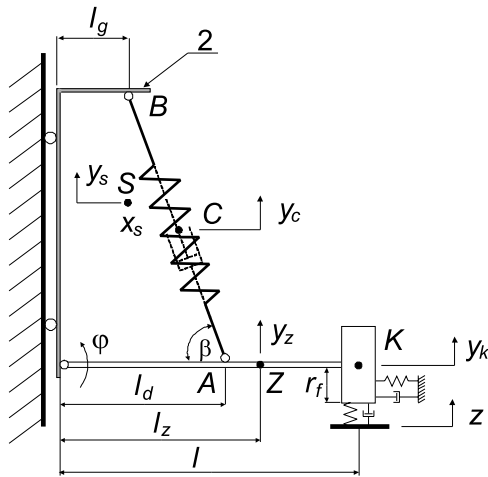


Fig. 2. Model of the quarter car

The assumed model is a common model of a quarter car with its suspension elements. Moveable frame 2, which represents the quarter of a car body, should be protected from vibrations transmitted from the wheel. The set of elements which mass centre is located in point Z consists of: a wheel, a brake disc, a steering knuckle, a suspension arm, and a wheel hub. The total mass of these elements is assigned as  $m_z$ . A spring and a damper were placed in parallel arrangement between the suspension arm and the moveable frame 2. The mass centre of these elements is depicted in point C, placed half-way between the endpoints of the line segment AB. Dynamic properties of the spring and the damper are described by a stiffness coefficient  $c_z$  and a damping coefficient  $b_z$ . Dynamic properties of the wheel are described by: stiffness coefficients  $c_k$   $c_{kv}$  and damping coefficients  $b_k$   $b_{kv}$ . In order to decrease disadvantageous dynamic effects of the system the mass centre S of the frame 2 was assumed to be placed on the same vertical line as an upper fixing point B of the suspension. The angle  $\beta$  was assumed to be constant.

Parameters of the system, used in calculations, were carried out as well as derived from the literature (Hansen 1997). Final model parameters set is presented in the Table 1.

Table 1

Suspension system parameters

No	Symbol	Value
1	$m_s$	300 [kg]
2	$m_z$	34.14 [kg]
3	$m_c$	6.28 [kg]
4	$I_z$	1.77 [kg m <sup>2</sup> ]
5	$l$	0.40 [m]
6	$l_z$	0.30 [m]
7	$l_d$	0.23 [m]
8	$l_l$	0.40 [m]
9	$l_g$	0.15 [m]
10	$r_f$	0.2 [m]
11	$x_s$	0.15 [m]
12	$c_z$	25000 [N/m]
13	$c_k$	180000 [N/m]
14	$c_{kv}$	100000 [N/m]
15	$b_z$	2200 [Ns/m]
16	$b_k$	500 [Ns/m]
17	$b_{kv}$	260 [Ns/m]
18	$\beta$	77 [deg]

### 3. STATIC AND DYNAMIC ANALYSIS

In this section both the static analysis and dynamic analysis of the system were carried out. In order to obtain the static components of reactions the system was divided into three subsystems as it is shown in Figure 3. It was assumed that the position of the system presented in Figure 2 and Figure 3 is its equilibrium position. Corresponding forces were applied to each of the subsystems.

The equations of equilibrium state were derived and solved. The results of calculations are presented in the Table 2.

The most significant forces, which will be used in designing process, are: the forces in linear bearings  $R_g$ ,  $R_d$  and the shaker force  $R_p$ . Forces in bearings have the same value, which is equal to 1955.4 [N]. Values of these forces will be used to select proper bearings. The value of the shaker force is necessary for designing of the electrohydraulic shaker.

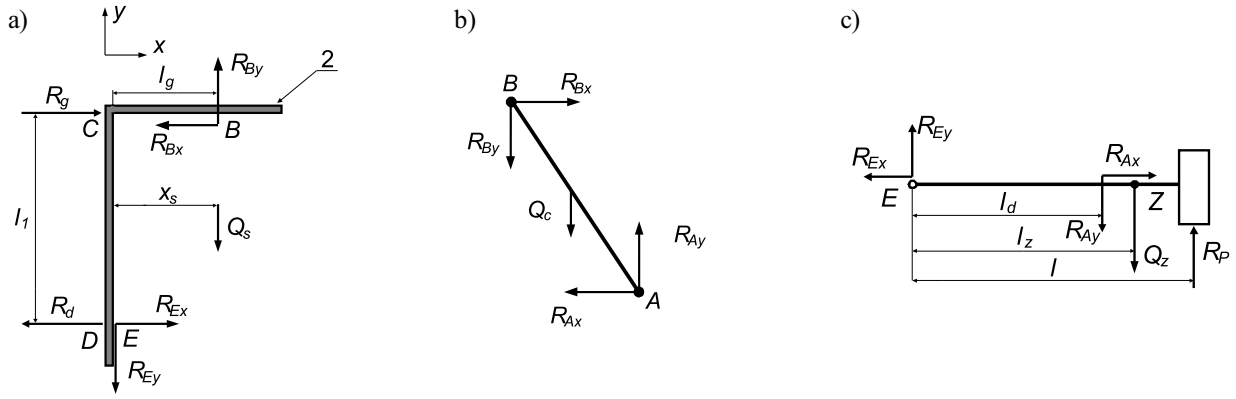


**Fig. 3.** Model for the static analysis: a) moveable frame 2; b) the bar which represents the spring and the damper of the car; c) the wheel with the suspension arm

**Table 2**  
Reactions in static equilibrium

Symbol	Location of reaction	Value [N]
$R_p$	shaker force	3339.5
$R_g, R_d$	force in linear bearing	1955.4
$R_{Ex}$	x component of the force in point E	1232.9
$R_{Ey}$	y component of the force in point E	2366.4
$R_{Bx}$	x component of the force in point B	1232.9
$R_{By}$	y component of the force in point B	5309.4

In order to perform some simulations of the motion, the equations of vibration were derived assuming the small displacements of the system. Admitting the generalized coordinates (in relation to the equilibrium position):  $y_s$  – vertical displacement of the frame 2,  $y_k$  – vertical displacement of the centre of the wheel, the following equations were derived:

$$\begin{cases}
 \left( m_s + m_z \frac{(l-l_z)^2}{l^2} + \frac{1}{4} m_c \frac{(2l-l_d)^2}{l^2} + \frac{I_z}{l^2} \right) \ddot{y}_s + \\
 + \left( m_z \frac{ll_z - l_z^2}{l^2} + \frac{1}{4} m_c \frac{2ll_d - l_d^2}{l^2} - \frac{I_z}{l^2} \right) \ddot{y}_k + \\
 + \left( b_z \frac{l_d^2 \sin^2 \beta}{l^2} + b_{kx} \frac{r_f^2}{l^2} \right) (\dot{y}_s - \dot{y}_k) + \\
 + \left( c_z \frac{l_d^2 \sin^2 \beta}{l^2} + c_{kx} \frac{r_f^2}{l^2} \right) (y_s - y_k) = 0 \\
 \left( m_z \frac{l_z^2}{l^2} + \frac{1}{4} m_c \frac{l_d^2}{l^2} + \frac{I_z}{l^2} \right) \ddot{y}_k + \\
 + \left( m_z \frac{ll_z - l_z^2}{l^2} + \frac{1}{4} m_c \frac{2ll_d - l_d^2}{l^2} - \frac{I_z}{l^2} \right) \ddot{y}_s + b_k \dot{y}_k + \\
 + \left( b_z \frac{l_d^2 \sin^2 \beta}{l^2} + b_{kx} \frac{r_f^2}{l^2} \right) (\dot{y}_k - \dot{y}_s) + c_k y_k + \\
 + \left( c_z \frac{l_d^2 \sin^2 \beta}{l^2} + c_{kx} \frac{r_f^2}{l^2} \right) (y_k - y_s) = b_k \dot{z} + c_k z
 \end{cases} \quad (1)$$

For the considered system the modal analysis was carried out. The first and the second natural frequencies of the system without damping are equal to  $f_1 = 1.49$  [Hz],  $f_2 = 13.24$  [Hz], and the corresponding modal vectors are as follows:  $[1; 0.15]$  and  $[-0.0044; 1]$ . The natural frequencies of the system with damping are equal to  $f_1 = 1.46$  [Hz],  $f_2 = 5.63$  [Hz]. Simple analysis of modal vector components shows that the displacement  $y_s$  is dominant when the system executes the vibration with the first mode.

In the next stage, the dynamic components of reactions were calculated. The scheme of forces used in calculations is shown in Figure 4. Except the gravitational forces and reactions, the inertial forces  $B_s, B_c, B_z$  and moment  $M_z$  are depicted in the scheme.

The reactions, including static and dynamic components, were derived using kinetostatic method.

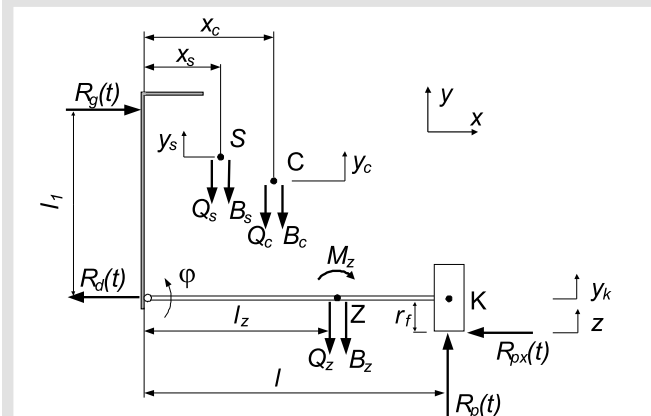


**Fig. 4.** Scheme of forces taken into account in calculations

#### 4. RESULTS OF SIMULATIONS

Simulations were carried out for various kinematic excitations. Selected results of calculations are presented graphically in Figures 5–14. The chirp signal was used as an excitation signal  $z(t)$  in the first stage of the simulations. The frequency increases in a linear manner from 0 to 20 [Hz] in time

range of 25 [s] as shown in Figure 5. Exemplary excitation time history is presented in Figure 6. The bandwidth of the input signal was based on the assumption that the vehicle body vibrations are characterized by a bandwidth around 1–5 [Hz] and the wheel vibrations are concentrated around 12–18 [Hz] (Savaresi 2010). The time histories of displacements  $y_s$  and  $y_k$  are shown in Figures 7 and 8. The time history of shaker force is shown in Figure 9.

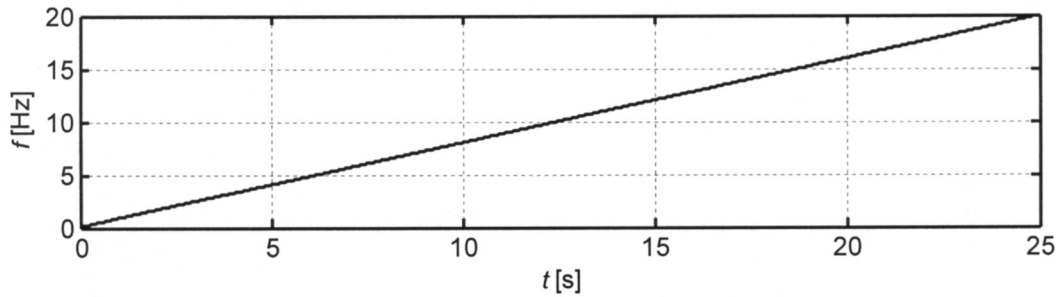


Fig. 5. Frequency of excitation as a function of time

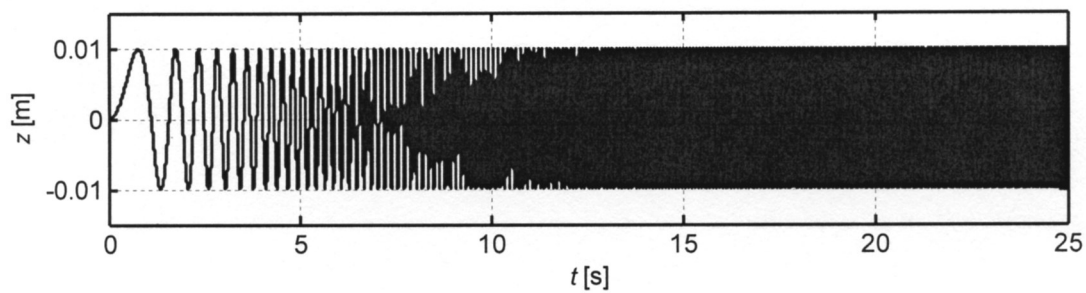


Fig. 6. Time history of kinematic excitation

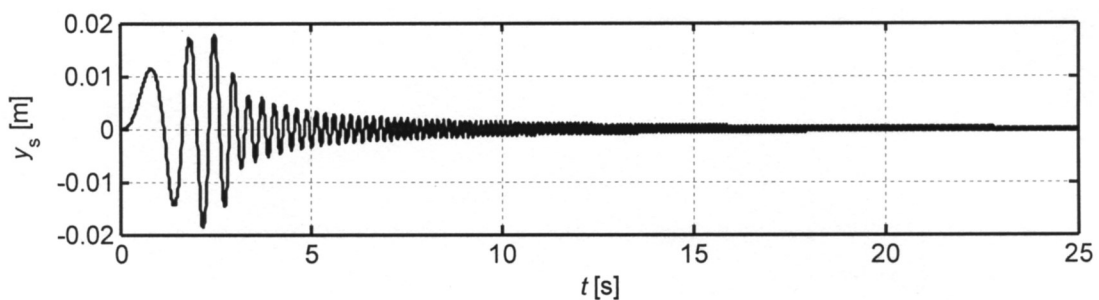


Fig. 7. Time history of the frame displacement

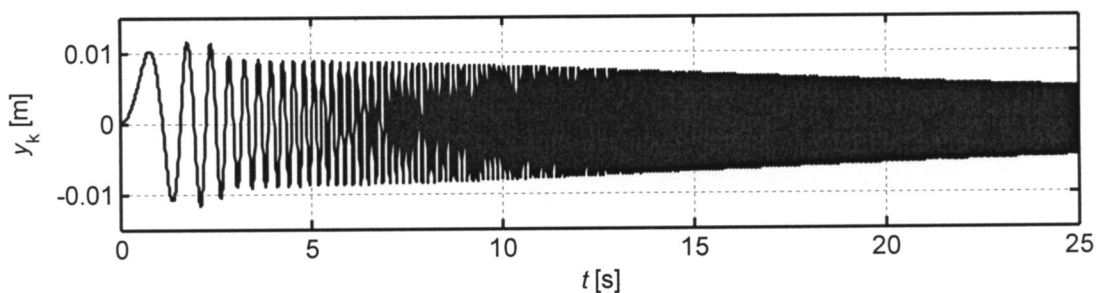


Fig. 8. Time history of the wheel displacement

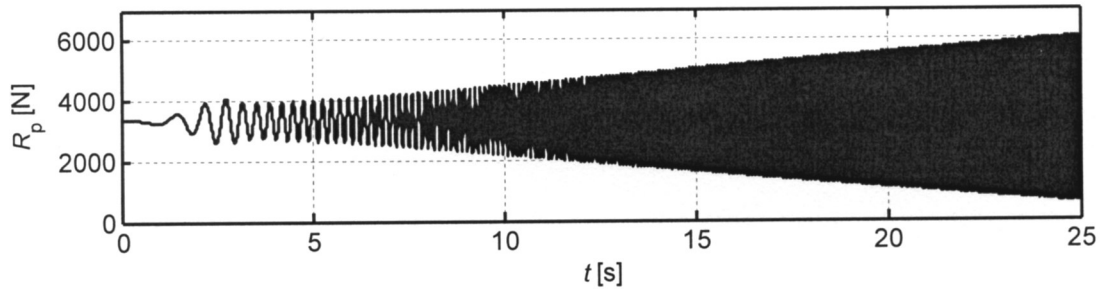


Fig. 9. Time course of the shaker force  $R_p$

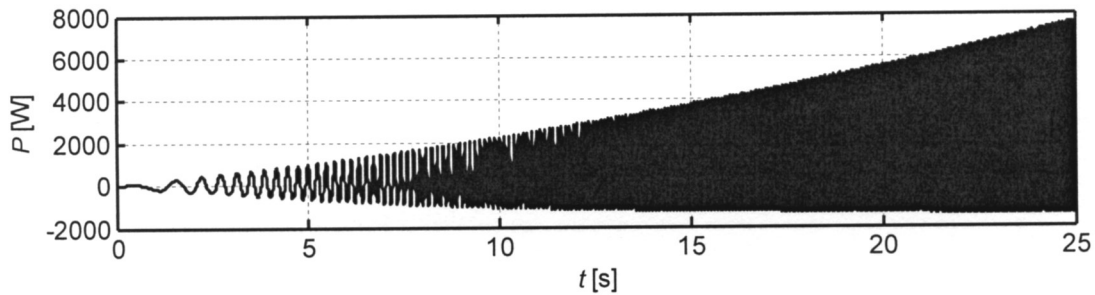


Fig. 10. Time history of the power transmitted from the shaker to the wheel

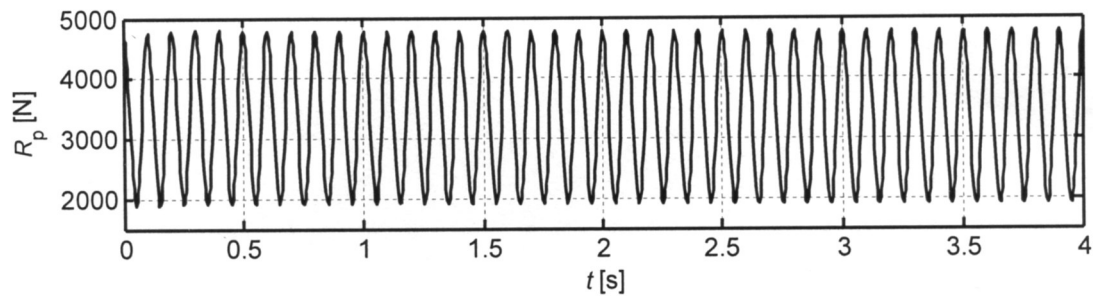


Fig. 11. Time history of the shaker force  $R_p$  for sinusoidal input signal

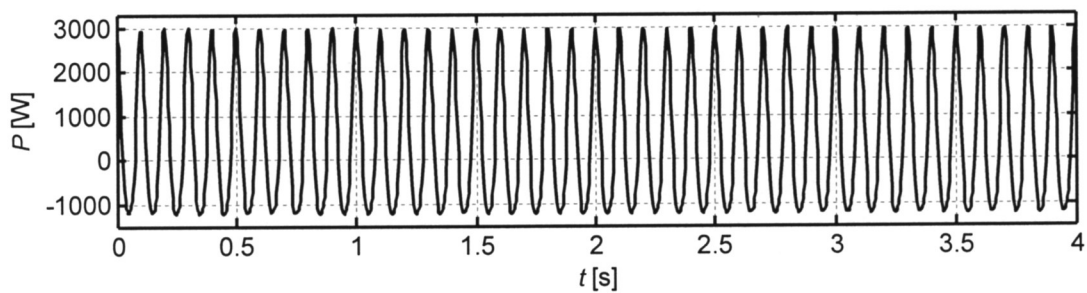


Fig. 12. Time history of the power transmitted from the shaker to the wheel for sinusoidal input signal

One of the primary parameters of the electrohydraulic shaker is the power which can be delivered to the system. Power transferred from the electrohydraulic shaker to the suspension system was determined and example results are shown in Figure 10 and 12. The time history of power presented in the Figure 12 and the shaker force shown in Figure 11 were obtained for sinusoidal excitation. Frequency of

the excitation was equal to 10 [Hz] and the amplitude was equal to 10 [mm]. Additionally the average power ( $P_{av}$ ) was calculated. The maximal values and the average values of power are presented in the Table 3. The further increasing the frequency and amplitude of excitation can lead to loss of contact between the wheel and the shaker. The transmissibility ratios of the system are shown in Figures 13 and 14.

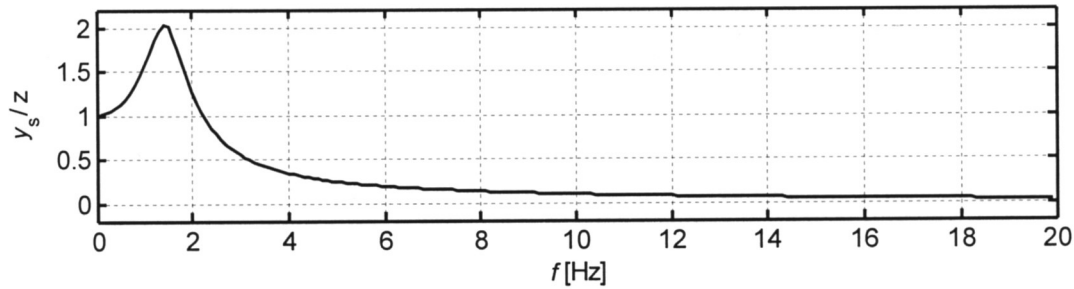


Fig. 13. Transmissibility ratio of frame displacement to the kinematic excitation

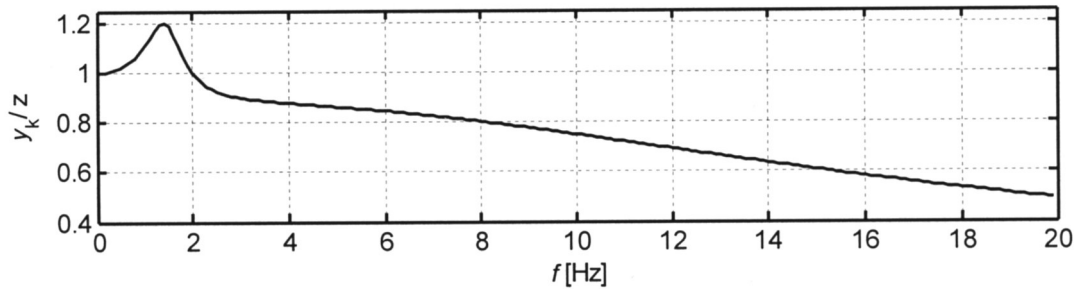


Fig. 14. Transmissibility ratio of wheel displacement to the kinematic excitation

Table 3

The average value  $P_{av}$  and maximal values  $P_{max}$  of power

$f$ [Hz]	Amplitude [mm]	$P_{av}$ [W]	$P_{max}$ [W]
1	5	0.38	105.5
	10	1.51	212
1.4	5	3.88	155
	10	15.54	325
2	5	9.98	230
	10	40	500
4	5	20	460
	10	82	1000
6	5	41	700
	10	166	1600
8	5	72	980
	10	289	2250
10	5	112	1250
	10	450	3000
12	5	161	1560
	10	645	3775
14	5	218	1890
	10	871	4648
16	5	281	2240
	10	1130	5600
18	5	352	2600
	10	1400	6600

## 5. CONCLUSIONS

In this paper assumptions and calculations of the new laboratory stand for testing car suspensions were presented. On the basis of calculations the following conclusions can be formulated:

- The static reactions in linear bearings are equal to 1955.4 [N]
- The largest values of shaker force  $R_p$  is about 6000 [N].
- The maximal value of the transmissibility ratio of frame displacement to kinematic excitation is equal to 2. This va-

lue was achieved for the frequency of excitation equal to the first natural frequency of the system. The influence of the second resonance of the frame motion is negligible.

- The largest value of the average power calculated for sinusoidal excitation is equal to 1400 [W] and the maximal value of the power is equal to 6600 [W]. These values were achieved for the maximal value of frequency.

All results will help to design mechanical part of the laboratory setup as well as the electrohydraulic shaker. The final project of the laboratory stand requires other calculations e.g. strength calculations of the frame construction.

## Acknowledgement

This study is a part of the research project no N N502213938

## References

- Hansen C.H., Snyder S.D. 1997, *Active Control of Noise and Vibration*. E&FN SPON Chapman & Hall, London SE1 8HN, UK.
- Korp D. 1998, *Ford Focus. Poradnik Użytkownika*. Wydawnictwa Komunikacji i Łączności, Warszawa.
- Langdon J.D. 2007, *Design and Adaptive Control of a Lab-based, Tire-coupled, Quarter-car Suspension Test Rig for the Accurate Re-creation of Vehicle Response*. Danville, VA.
- Mohd R.B.A. 2008, *Simulation and Experimental Analysis of an Active Vehicle Suspension System*. Faculty of Mechanical Engineering Universiti Teknologi Malaysia 2007.
- Reimpel J., Betzler J. 2000, *Podwozia samochodów. Podstawy konstrukcji*. Wydawnictwa Komunikacji i Łączności, Warszawa 2000.
- Savaresi S.M., Poussot-Vassal C., Spelta C., Sename O., Dugard L. 2010, *Semi-Active Suspension Control Design for Vehicles*. Elsevier.
- Yoshimura T., Kume A., Kurimoto M., Himo J. 2001, *Construction of an active suspension system of a quarter car model using the concept of sliding mode control*. Journal of Sound and Vibration, 239(2), 187–199.
- Teramura I., Yoshimura T. 2005, *Active suspension control of a one-wheel car model using single input rule modules fuzzy reasoning and a disturbance observer*. Journal of Zhejiang University Science, ISSN 1009-3095.